



# IJRASET

International Journal For Research in  
Applied Science and Engineering Technology



---

# INTERNATIONAL JOURNAL FOR RESEARCH

IN APPLIED SCIENCE & ENGINEERING TECHNOLOGY

---

**Volume:** 10    **Issue:** IX    **Month of publication:** September 2022

**DOI:** <https://doi.org/10.22214/ijraset.2022.46333>

[www.ijraset.com](http://www.ijraset.com)

Call:  08813907089

E-mail ID: [ijraset@gmail.com](mailto:ijraset@gmail.com)

# Spectral and FTIR Analysis of Dy<sup>3+</sup> ions doped Zinc Lithium Cadmium Magnesium Borophosphate Glasses

S. L. Meena

Ceramic Laboratory, Department of physics, Jai Narain Vyas University, Jodhpur 342001(Raj) India

**Abstract:** Glass of the system:  $(40-x) P_2O_5:10ZnO:10Li_2O:10CdO:10MgO:20B_2O_3: xDy_2O_3$ . (where  $x=1, 1.5, 2$  mol %) have been prepared by melt-quenching method. (where  $x=1, 1.5$  and  $2$  mol%) have been prepared by melt-quenching technique. The amorphous nature of the prepared glass samples was confirmed by X-ray diffraction. Optical absorption, Excitation, fluorescence and FTIR spectra have been recorded at room temperature for all glass samples. Judd-Ofelt intensity parameters  $\Omega_\lambda$  ( $\lambda=2, 4$  and  $6$ ) are evaluated from the intensities of various absorption bands of optical absorption spectra. Using these intensity parameters various radiative properties like spontaneous emission probability, branching ratio, radiative life time and stimulated emission cross-section of various emission lines have been evaluated.

**Keywords:** ZLCMBP Glasses, Optical Properties, Judd-Ofelt Theory, Transmittance Properties

## I. INTRODUCTION

Glasses are receiving considerable attention due to their potential application in optical devices such as frequency-conversion materials, laser action and optical fiber amplifiers [1-5]. Among different host matrices, phosphate glasses have wide range of applications in the field of glass ceramics, with the advantages such as low non-linear refractive index, good physical and chemical stability and high transparency from near Ultra Violet to mid-Infrared region [6-10]. Phosphate glasses have relatively low phonon energy and exhibit better environment resistance.

Additionally, such glasses are characterized by a high capacity for dissolving rare earth elements. The chemical resistance and transparency of phosphate glasses were investigated to obtain glasses with optical transparency. These glasses are also stable [11]. Recently, glass-ceramics containing dysprosium oxides have been found in applications for several different purposes. Dy<sup>3+</sup> doped glasses have attracted much interest due to their important optical properties used in lasers, optical amplifiers, photonic devices and as infrared sensors [12-15].

The present work reports on the preparation and characterization of rare earth doped heavy metal oxide (HMO) glass systems for lasing materials. I have studied on the absorption and emission properties of Dy<sup>3+</sup> doped zinc lithium cadmium magnesium borophosphate glasses. The intensities of the transitions for the rare earth ions have been estimated successfully using the Judd-Ofelt theory, The laser parameters such as radiative probabilities(A), branching ratio ( $\beta$ ), radiative life time( $\tau_R$ ) and stimulated emission cross section( $\sigma_p$ ) are evaluated using J.O.intensity parameters( $\Omega_\lambda$ ,  $\lambda=2, 4$  and  $6$ ).

## II. EXPERIMENTAL TECHNIQUES

### A. Preparation of Glasses

The following Dy<sup>3+</sup>doped phosphate glass samples  $(40-x) P_2O_5:10 ZnO: 10Li_2O:10 CdO: 10MgO: 20B_2O_3: xDy_2O_3$ . (where  $x=1, 1.5$  and  $2$  mol %) have been prepared by melt-quenching method. Analytical reagent grade chemical used in the present study consist of  $P_2O_5$ , ZnO,  $Li_2O$ , CdO, MgO,  $B_2O_3$  and  $Dy_2O_3$ . They were thoroughly mixed by using an agate pestle mortar. then melted at  $1052^\circ C$  by an electrical muffle furnace for 2h., After complete melting, the melts were quickly poured in to a preheated stainless steel mould and annealed at temperature of  $250^\circ C$  for 2h to remove thermal strains and stresses. Every time fine powder of cerium oxide was used for polishing the samples. The glass samples so prepared were of good optical quality and were transparent. The chemical compositions of the glasses with the name of samples are summarized in **Table 1**.

Table 1.

Chemical composition of the glasses

Sample	Glass composition (mol %)
ZLCMBP (UD)	40 P <sub>2</sub> O <sub>5</sub> :10ZnO:10Li <sub>2</sub> O:10CdO:10MgO:20B <sub>2</sub> O <sub>3</sub>
ZLCMBP (DY1)	39 P <sub>2</sub> O <sub>5</sub> :10ZnO:10Li <sub>2</sub> O:10 CdO: 10 MgO: 20 B <sub>2</sub> O <sub>3</sub> : 1 Dy <sub>2</sub> O <sub>3</sub> .
ZLCMBP (DY1.5)	38.5P <sub>2</sub> O <sub>5</sub> :10ZnO:10Li <sub>2</sub> O:10 CdO: 10 MgO: 20 B <sub>2</sub> O <sub>3</sub> : 1.5 Dy <sub>2</sub> O <sub>3</sub> .
ZLCMBP (DY2)	38 P <sub>2</sub> O <sub>5</sub> :10ZnO:10Li <sub>2</sub> O:10 CdO: 10 MgO: 20 B <sub>2</sub> O <sub>3</sub> : 2 Dy <sub>2</sub> O <sub>3</sub> .
ZLCMBP (UD)	-Represents undoped Zinc Lithium Cadmium Magnesium Borophosphate glass specimen
ZLCMBP (DY)	-Represents Dy <sup>3+</sup> doped Zinc Lithium Cadmium Magnesium Borophosphate glass specimens.

### III. THEORY

#### A. Oscillator Strength

The intensity of spectral lines are expressed in terms of oscillator strengths using the relation [16].

$$f_{\text{expt.}} = 4.318 \times 10^{-9} \int \epsilon(\nu) d\nu \tag{1}$$

where,  $\epsilon(\nu)$  is molar absorption coefficient at a given energy  $\nu$  (cm<sup>-1</sup>), to be evaluated from Beer–Lambert law.

Under Gaussian Approximation, using Beer–Lambert law, the observed oscillator strengths of the absorption bands have been experimentally calculated [17], using the modified relation:

$$P_m = 4.6 \times 10^{-9} \times \frac{1}{cl} \log \frac{I_0}{I} \times \Delta\nu_{1/2} \tag{2}$$

where  $c$  is the molar concentration of the absorbing ion per unit volume,  $l$  is the optical path length,  $\log I_0/I$  is optical density and  $\Delta\nu_{1/2}$  is half band width.

#### B. Judd-Ofelt Intensity Parameters

According to Judd [18] and Ofelt [19] theory, independently derived expression for the oscillator strength of the induced forced electric dipole transitions between an initial  $J$  manifold  $|4f^N(S, L) J\rangle$  level and the terminal  $J'$  manifold  $|4f^N(S', L') J'\rangle$  is given by:

$$\frac{8\pi^2 m c \bar{\nu}}{3h(2J+1)n} \left[ \frac{(n^2+2)^2}{9} \right] \times S(J, J') \tag{3}$$

Where,

the line strength  $S(J, J')$  is given by the equation

$$S(J, J') = e^2 \sum_{\lambda=2,4,6} \Omega_{\lambda} \langle 4f^N(S, L) J \| U^{(\lambda)} \| 4f^N(S', L') J' \rangle^2 \tag{4}$$

In the above equation  $m$  is the mass of an electron,  $c$  is the velocity of light,  $\nu$  is the wave number of the transition,  $h$  is Planck's constant,  $n$  is the refractive index,  $J$  and  $J'$  are the total angular momentum of the initial and final level respectively,  $\Omega_{\lambda}$  ( $\lambda=2,4$  and  $6$ ) are known as Judd-Ofelt intensity parameters.

#### C. Radiative Properties

The  $\Omega_{\lambda}$  parameters obtained using the absorption spectral results have been used to predict radiative properties such as spontaneous emission probability ( $A$ ) and radiative life time ( $\tau_R$ ), and laser parameters like fluorescence branching ratio ( $\beta_R$ ) and stimulated emission cross section ( $\sigma_p$ ).

The spontaneous emission probability from initial manifold  $|4f^N(S', L') J'\rangle$  to a final manifold  $|4f^N(S, L) J\rangle$  is given by:

$$A[(S', L') J'; (S, L) J] = \frac{64 \pi^2 \nu^3}{3h(2J'+1)} \left[ \frac{n(n^2+2)^2}{9} \right] \times S(J', J) \tag{5}$$

Where,  $S(J', J) = e^2 [\Omega_2 \| U^{(2)} \|^2 + \Omega_4 \| U^{(4)} \|^2 + \Omega_6 \| U^{(6)} \|^2]$

The fluorescence branching ratio for the transitions originating from a specific initial manifold  $|4f^N(S', L') J' \rangle$  to a final many fold  $|4f^N(S, L) J \rangle$  is given by

$$\beta [(S', L') J'; (S, L) J] = \frac{A[(S', L') J'; (S, L) J]}{\sum_{S, L, J} A[(S', L') J'; (S, L) J]} \quad (6)$$

where, the sum is over all terminal manifolds.

The radiative life time is given by

$$\tau_{rad} = \frac{1}{\sum_{S, L, J} A[(S', L') J'; (S, L) J]} = A_{Total}^{-1} \quad (7)$$

where, the sum is over all possible terminal manifolds. The stimulated emission cross-section for a transition from an initial manifold  $|4f^N(S', L') J' \rangle$  to a final manifold  $|4f^N(S, L) J \rangle$  is expressed as

$$\sigma_p(\lambda_p) = \left[ \frac{\lambda_p^4}{8\pi c n^2 \Delta\lambda_{eff}} \right] \times A[(S', L') J'; (S, L) J] \quad (8)$$

where,  $\lambda_p$  the peak fluorescence wavelength of the emission band and  $\Delta\lambda_{eff}$  is the effective fluorescence line width.

#### IV. RESULT AND DISCUSSION

##### A. XRD Measurement

Figure 1 presents the XRD pattern of the sample contain -  $P_2O_5$  which is show no sharp Bragg's peak, but only a broad diffuse hump around low angle region. This is the clear indication of amorphous nature within the resolution limit of XRD instrument.

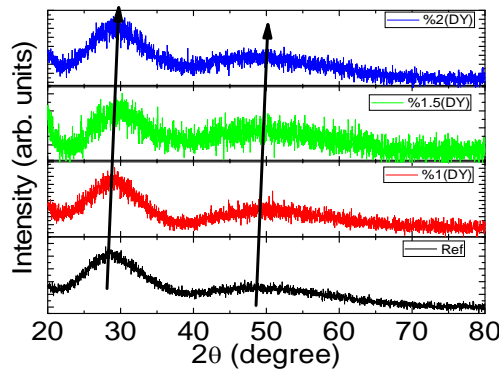


Fig. (1) X-ray diffraction pattern of  $P_2O_5:ZnO:Li_2O:CaO:MgO:B_2O_3:Dy_2O_3$ .

##### B. FTIR Transmission Spectra

The FTIR spectrum of ZLCMBP (DY 01) glass is in the wave number range  $500-2500\text{ cm}^{-1}$  is presented in Fig.2 and the possible mechanism bands are tabulated in Table 2.

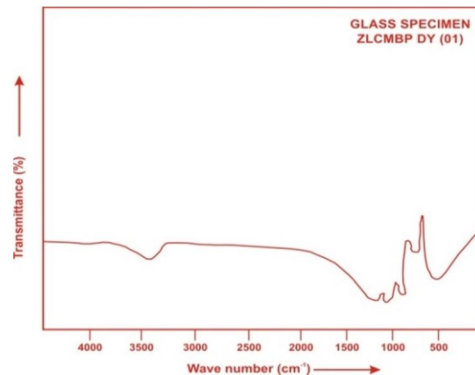


Fig. (2) FTIR spectrum of ZLCMBP DY (01) glass.



The band observed at  $525\text{ cm}^{-1}$  is attributed to the P-O-P bending vibrations [20]. The observed band around at  $750\text{ cm}^{-1}$  is due to the P-O-P symmetric stretching vibrations while the occurrence of band around  $925\text{ cm}^{-1}$  is assigned to the P-O-P asymmetric stretching vibrations [21, 22]. The Asymmetric stretching modes of  $(\text{PO}_3)^{2-}$  groups is observed around  $1110\text{ cm}^{-1}$ [23]. The Asymmetric stretching vibration of P=O and O-P-O bonds is observed around  $1234\text{ cm}^{-1}$ [24]. The observed band around at  $3425\text{ cm}^{-1}$  is attributed to symmetric stretching vibrations of the O-H bonds [25].

Table2. Assignment of infrared transmission bands of (ZLCMBP DY 01) glass.

Peak position( $\text{cm}^{-1}$ )	Band Assignment
~ 525	Bending vibration of P-O-P bands
~750	Symmetric stretching vibration of P-O-P bonds
~925	Asymmetric stretching vibration of P-O-P bonds
~1110	Asymmetric stretching modes of $(\text{PO}_3)^{2-}$ groups
~1234	Asymmetric Stretching Vibration of P=O and O-P-O bonds
~3425	Symmetric stretching of the O-H bonds

### C. Absorption Spectrum

The absorption spectra of  $\text{Dy}^{3+}$  doped ZLCMBP glass specimens have been presented in Figure 3 in terms of Intensity versus wavelength. Thirteen absorption bands have been observed from the ground state  $^6\text{H}_{15/2}$  to excited states  $^6\text{H}_{13/2}$ ,  $^6\text{H}_{11/2}$ ,  $^6\text{H}_{9/2}+^6\text{F}_{11/2}$ ,  $^6\text{H}_{7/2}+^6\text{F}_{9/2}$ ,  $^6\text{F}_{7/2}+^6\text{H}_{5/2}$ ,  $^6\text{F}_{5/2}$ ,  $^6\text{F}_{3/2}$ ,  $^6\text{F}_{9/2}$ ,  $^4\text{I}_{15/2}$ ,  $^4\text{G}_{11/2}$ ,  $^6\text{F}_{7/2}+^4\text{I}_{13/2}$ ,  $^6\text{M}_{19/2}+4(\text{P,D})_{3/2}$  and  $^4\text{G}_{9/2}+^6\text{P}_{3/2}$  for  $\text{Dy}^{3+}$  doped ZLCMBP glasses.

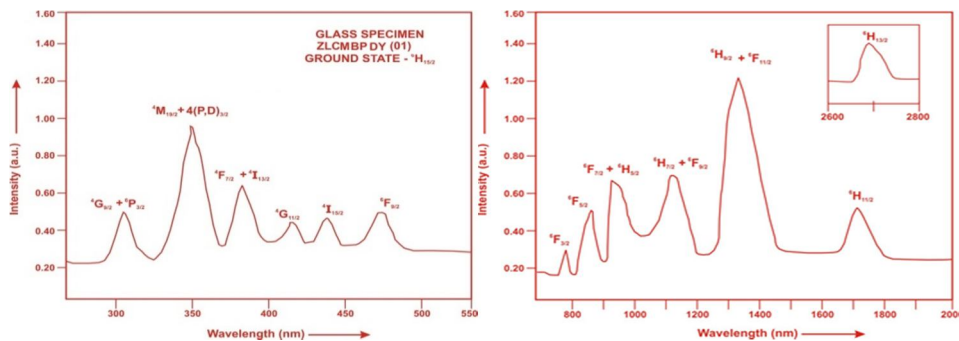


Fig. (3) Absorption spectrum of ZLCMBP DY (01) glass.

The experimental and calculated oscillator strength for  $\text{Dy}^{3+}$  ions in ZLCMBP glasses are given in **Table 3**.

Table 3: Measured and calculated oscillator strength ( $P_m \times 10^{+6}$ ) of  $\text{Dy}^{3+}$  ions in ZLCMBP glasses.

Energy level from $^6\text{H}_{15/2}$	Glass ZLCMBP (DY01)		Glass ZLCMBP (DY1.5)		Glass ZLCMBP (DY02)	
	$P_{\text{exp}}$	$P_{\text{cal}}$	$P_{\text{exp}}$	$P_{\text{cal}}$	$P_{\text{exp}}$	$P_{\text{cal}}$
$^6\text{H}_{13/2}$	2.02	2.37	2.00	2.34	1.98	2.35
$^6\text{H}_{11/2}$	1.38	1.96	1.36	1.94	1.33	1.92
$^6\text{H}_{9/2}+^6\text{F}_{11/2}$	10.21	10.10	10.19	10.08	10.17	10.06
$^6\text{H}_{7/2}+^6\text{F}_{9/2}$	5.52	5.21	5.50	5.19	5.47	5.16
$^6\text{F}_{7/2}+^6\text{H}_{5/2}$	4.67	3.67	4.65	3.64	4.63	3.60
$^6\text{F}_{5/2}$	1.28	1.64	1.27	1.62	1.25	1.60
$^6\text{F}_{3/2}$	0.27	0.31	0.26	0.31	0.24	0.30
$^6\text{F}_{9/2}$	0.31	0.28	0.30	0.28	0.28	0.27
$^4\text{I}_{15/2}$	0.29	0.68	0.28	0.67	0.26	0.66
$^4\text{G}_{11/2}$	0.21	0.17	0.20	0.17	0.19	0.17
$^6\text{F}_{7/2}+^4\text{I}_{13/2}$	3.40	3.62	3.38	3.60	3.35	3.35
$^6\text{M}_{19/2}+4(\text{P,D})_{3/2}$	7.93	10.03	7.91	10.01	7.89	10.00
$^4\text{G}_{9/2}+^6\text{P}_{3/2}$	1.58	2.03	1.56	2.02	1.53	2.00
r.m.s. deviation	0.70697		0.71054		0.71763	

In the Zinc Lithium Cadmium Magnesium Borophosphate glasses  $\Omega_2$ ,  $\Omega_4$  and  $\Omega_6$  parameters decrease with the increase of x from 1 to 2 mol%. The order of magnitude of Judd-Ofelt intensity parameters is  $\Omega_2 > \Omega_4 > \Omega_6$  for all the glass specimens. The spectroscopic quality factor ( $\Omega_4 / \Omega_6$ ) related with the rigidity of the glass system has been found to lie between 1.247 and 1.287 in the present glasses.

The values of Judd-Ofelt intensity parameters are given in **Table 4**.

Table 4: Judd-Ofelt intensity parameters for Dy<sup>3+</sup> doped ZLCMBP glass specimens.

Glass Specimen	$\Omega_2(\text{pm}^2)$	$\Omega_4(\text{pm}^2)$	$\Omega_6(\text{pm}^2)$	$\Omega_4 / \Omega_6$	Ref.
ZLCMBP (DY01)	2.801	1.711	1.372	1.247	P.W.
ZLCMBP (DY1.5)	2.790	1.714	1.355	1.265	P.W.
ZLCMBP (DY02)	2.779	1.720	1.336	1.287	P.W.
NSGP(DY)	12.38	6.31	3.20	1.972	[26]
ZP(DY)	2.483	0.950	0.673	1.412	[27]
LLPNBP(SM)	5.152	4.553	4.198	1.085	[28]
LLCTMBB(DY)	2.457	1.471	1.116	1.318	[29]
ZLCBP(SM)	4.599	4.096	3.813	1.074	[30]

#### D. Excitation Spectrum

The Excitation spectra of Dy<sup>3+</sup>doped ZLCMBP glass specimen has been presented in Figure 4 in terms of Excitation Intensity versus wavelength. The excitation spectrum was recorded in the spectral region 315–465 nm fluorescence at 575nm having different excitation band centered at 322,353, 365, 385, 425, 454 and 473 nm are attributed to the <sup>6</sup>P<sub>3/2</sub>, <sup>6</sup>P<sub>7/2</sub>, <sup>4</sup>P<sub>3/2</sub>, <sup>4</sup>I<sub>13/2</sub>, <sup>4</sup>G<sub>11/2</sub>, <sup>4</sup>I<sub>15/2</sub> and <sup>4</sup>F<sub>9/2</sub> transitions, respectively. The highest absorption level is <sup>4</sup>I<sub>13/2</sub> and is at 385nm. So this is to be chosen for excitation wavelength.

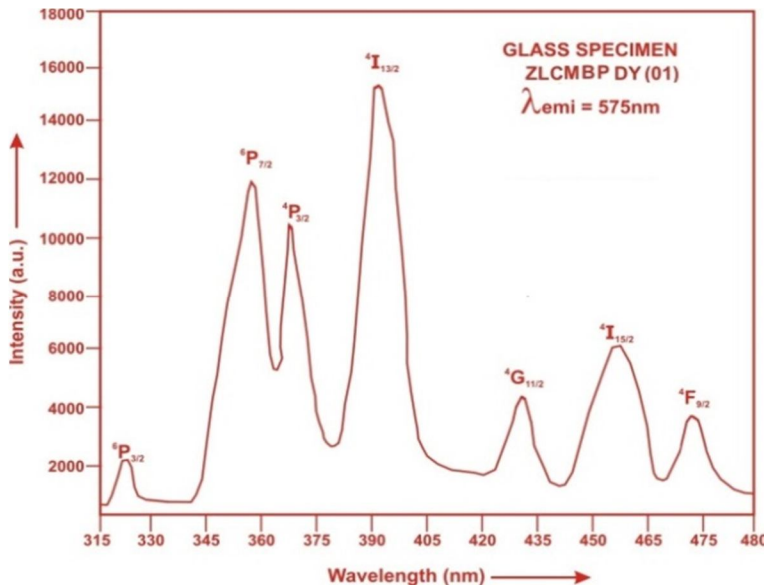


Fig. (4) Excitation spectrum of ZLCMBP DY (01) glass.

#### E. Fluorescence Spectrum

The Fluorescence spectrum of Dy<sup>3+</sup>doped in Zinc Lithium Cadmium Magnesium Borophosphate glass is shown in Figure 5. There are four broad bands observed in the Fluorescence spectrum of Dy<sup>3+</sup>doped Zinc Lithium Cadmium Magnesium Borophosphate glass. The wavelengths of these bands along with their assignments are given in Table 4. The peak with maximum emission intensity appears at 485nm, 575 nm, 665 nm and 752 nm corresponds to the (<sup>4</sup>F<sub>9/2</sub>→<sup>6</sup>H<sub>15/2</sub>), (<sup>4</sup>F<sub>9/2</sub>→<sup>6</sup>H<sub>13/2</sub>), (<sup>4</sup>F<sub>9/2</sub>→<sup>6</sup>H<sub>11/2</sub>) and (<sup>4</sup>F<sub>9/2</sub>→<sup>6</sup>H<sub>9/2</sub>) transition.

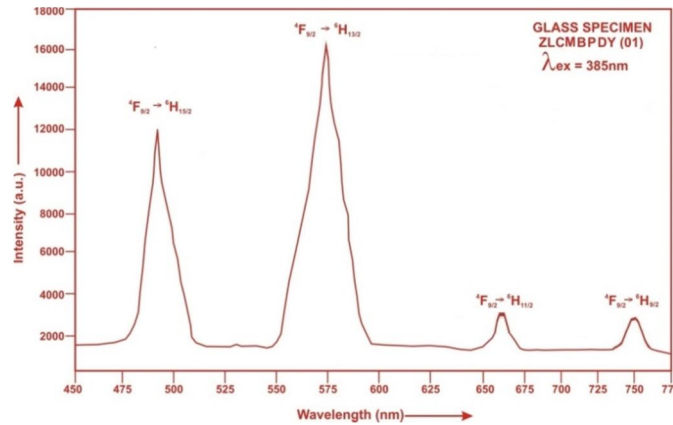


Fig. (5). Fluorescence spectrum of ZLCMBP DY (01) glass.

Table5: Emission peak wave lengths ( $\lambda_p$ ),radiative transition probability ( $A_{rad}$ ),branching ratio ( $\beta$ ),stimulated emission cross-section( $\sigma_p$ ) and radiative life time( $\tau_R$ ) for various transitions in Dy<sup>3+</sup> doped ZLCMBP glasses.

Transition	ZLCMBP DY 01					ZLCMBP DY 1.5				ZLCMBP DY 02			
	$\lambda_{max}$ (nm)	$A_{rad}(s^{-1})$	$\beta$	$\sigma_p$ ( $10^{-20}$ $cm^2$ )	$\tau_R(\mu s)$	$A_{rad}(s^{-1})$	$\beta$	$\sigma_p$ ( $10^{-20}$ $cm^2$ )	$\tau_R(\mu s)$	$A_{rad}(s^{-1})$	$\beta$	$\sigma_p$ ( $10^{-20}$ $cm^2$ )	$\tau_R$ ( $10^{-20}$ $cm^2$ )
${}^4F_{9/2} \rightarrow {}^6H_1$ 5/2	485	79.70	0.1967	0.168	2468.0 6	79.01	0.1959	0.164	2479.6 2	78.33	0.1951	0.159	2490.68
${}^4F_{9/2} \rightarrow {}^6H_1$ 3/2	575	273.64	0.6753	1.239		272.57	0.6759	1.212		271.56	0.6764	1.185	
${}^4F_{9/2} \rightarrow {}^6H_1$ 1/2	665	28.93	0.0714	0.145		28.86	0.0716	0.143		28.78	0.0717	0.141	
${}^4F_{9/2} \rightarrow {}^6H_9$ 2	752	22.91	0.0565	0.136		22.86	0.0567	0.134		22.82	0.0568	0.133	

### V. CONCLUSION

In the present study, the glass samples of composition  $(40-x) P_2O_5:10ZnO:10Li_2O:10CdO:10MgO:20B_2O_3 : xDy_2O_3$  (where  $x = 1, 1.5$  and  $2$  mol %) have been prepared by melt-quenching method. The value of stimulated emission cross-section ( $\sigma_p$ ) is found to be maximum for the transition ( ${}^4F_{9/2} \rightarrow {}^6H_{13/2}$ ) for all glass specimens. This shows that ( ${}^4F_{9/2} \rightarrow {}^6H_{13/2}$ ) transition is most probable transition. ). The FTIR of glasses revealed the presence of characteristic bonding vibrations of different functional groups.

### REFERENCES

- [1] Priyanka, R., Arunkumar, S., Basavapoornima, Ch., Mathelane, R.M. and Marimuthu, K.(2020). Structural and spectroscopic investigations on Eu<sup>3+</sup> ions doped boro-phosphate glasses for optical display applications. J. Lumin. 220, 116964.
- [2] Doerenkamp, C.,Carvajal, E., Magon, C.J., Faria, W.J.G.J., Pedro Donoso, J., Galvão Gobato, Y., de Camargo, A.S.S. and Eckert, H.(2019). Composition–structure–property correlations in rare-earth-doped heavy metal oxyfluoride glasses. J. Phys. Chem. C, 123, 22478–22490.
- [3] Seshadri, M., Radha, M., Barbosa, C., Cordeiro, C.M.B. and Ratnaka, Y.C.(2015). Effect of ZnO on spectroscopic properties of Sm<sup>3+</sup> doped zinc phosphate glasses,Physica B: Condensed matter 459, 79-87.
- [4] Vighnesh, K.R., Ramya, B., Nimitha, S., Wagh,A., Sayyed, M.I., Sakar, E., Yakout, H.A. and Dahshan, A. (2020).Structural, optical, thermal, mechanical, morphological and radiation shielding parameters of Pr<sup>3+</sup> doped ZAlFB glass systems, optical materials 99,109512.
- [5] Sontakke, Atul D., and Annapura, K. (2013).Spectroscopic properties and concentration effects on luminescence behavior of Nd<sup>3+</sup> doped Zinc– Boro– Bismuthate glasses, Mater. Chemi. Phys. 137, 916-921.
- [6] Rai, V.N., Raja Sekhar, B.N., Tiwari, P., Kshirsagar, R.J. and Deb, S.K. (2011).Spectroscopic studies of gama irradiated Nd<sup>3+</sup> doped phosphate Glasses, Journal of Non- crystalline soilds, 3757-3764.
- [7] Chowdhury,S., Mandal, P., and Ghosh, S.(2019). Structural properties of Er<sup>3+</sup> doped lead zinc phosphate glasses, Mat. Sci. and Eng.,240,116-120.
- [8] Yu, X., Duan, L., Ni, L. and Wang, Z. (2012).Fabrication and luminescence behavior of phosphate glass–ceramics co-doped with Er<sup>3+</sup> and Yb<sup>3+</sup>, Opt. Commun. 285, 3805–3808.
- [9] Milankovic, A.M., Gajovic, A. and Day, D.E. (2003).Spectroscopic investigation of MoO<sub>3</sub>–Fe<sub>2</sub>O<sub>3</sub>–P<sub>2</sub>O<sub>5</sub> and SrO–Fe<sub>2</sub>O<sub>3</sub>–P<sub>2</sub>O<sub>5</sub> glasses. J of Non-Crystalline Solids. 325:76-84.

- [10] Jiang, S., Myers, M. and Peyghambarian, N. (1998). Er<sup>3+</sup> doped phosphate glasses and lasers. *J. Non-Cryst. Solids*, 239, 143–148.
- [11] Aranha, N. (1994). Aranha. Niobium Phosphate Glasses: Preparation, Characterization, and Properties, PhD thesis, Unicamp.
- [12] Arul Rayappan, I., Maheshvaran, K., SurendraBabu, S. and Marimuthu, K. (2012). Dysprosium doped lead fluoroborate glasses: Structural, optical, and thermal investigations, *Phys. Status solid A.*, 209, 570-578.
- [13] Linganna, K., Rao, C.S. and Jayasankar, C.K. (2013). Optical properties and generation of white light in Dy<sup>3+</sup> doped lead phosphate glasses, *Journal of Quantitative Spectroscopy and Radiative Transfer*, 118, 40-48.
- [14] Pawar, P.P., Munishwar, S.R. and Gedam, R.S. (2017). Intense white light luminescent Dy<sup>3+</sup> doped lithium borate glasses for WLED: a correlation between physical, thermal, structural and optical properties. *Solid State Sci.*, 64, 41–50.
- [15] Pisarski, W.A., Zur, L. and Pisarska, J. (2011). Optical transitions of Eu<sup>3+</sup> and Dy<sup>3+</sup> ions in lead phosphate glasses. *Opt. Lett.*, 36, 990–992.
- [16] Gorller-Walrand, C. and Binnemans, K. (1988). Spectral Intensities of f-f Transition. In: Gshneider Jr., K.A. and Eyring, L., Eds., *Handbook on the Physics and Chemistry of Rare Earths*, Vol. 25, Chap. 167, North-Holland, Amsterdam, 101-264.
- [17] Sharma, Y.K., Surana, S.S.L. and Singh, R.K. (2009). Spectroscopic Investigations and Luminescence Spectra of Sm<sup>3+</sup> Doped Soda Lime Silicate Glasses. *Journal of Rare Earths*, 27, 773.
- [18] Judd, B.R. (1962). Optical Absorption Intensities of Rare Earth Ions. *Physical Review*, 127, 750.
- [19] Ofelt, G.S. (1962). Intensities of Crystal Spectra of Rare Earth Ions. *The Journal of Chemical Physics*, 37, 511.
- [20] Jha, P.K., Pandey, O.P., Singh, K. (2015). FTIR spectral analysis and mechanical properties of sodium phosphate glass-ceramics, *J. Mol. Struct.*, 1083, 278-285.
- [21] Pavia, D.L., Lampman, G.M., Kriz, G.S. and Vyvyan James (2009). *Introduction to Spectroscopy*, fourth eds., Books/Cole, Cengage Learning, USA.
- [22] Meyer, K. (1998). Characterization of the structure of binary zinc ultraphosphate glasses by infrared and Raman spectroscopy, *J. Non-Cryst. Solids*, 209, 227-239.
- [23] Le, Q.H., Palenta, T., Benzine, O., Griebenow, K., Limbach, R., Kamitsos, E.I., Wondraczek, L. (2017). Formation, structure and properties of fluoro-sulfo-phosphate polyanionic glasses, *J. Non-Cryst. Solids*, 477, 58-72.
- [24] Waclaawska, I., Szumera, M. and Sulowska, J. (2016). Structural characterization of zinc modified glasses from the SiO<sub>2</sub>-P<sub>2</sub>O<sub>5</sub>-K<sub>2</sub>O-CaO-MgO system, *J. Alloys Compd.* 666, 352-358.
- [25] Han, L., Zhang, J., Song, Z.I., Xiao, Y.C., Qiang, Y.C., Ye, X.Y., You, W.X. and Lu, A.X. (2020). A novel Eu<sup>3+</sup> doped phosphate glass for reddish orange emission: preparation, structure and fluorescence properties, *J. Lumin.*, 221, 117041. [3430].
- [26] Shoib, M., Chanthima, N., Rooh, G., Rajaramakrishna, R. and Kaewkhao, J. (2019). Physical and luminescence properties of rare earth doped phosphate glasses for solid state lighting applications, *Thai Int. Res.*, 14(3), 20-26.
- [27] Chandrasekhar, A. V., Radhapaty, A., Reddy, B.J., Reddy, Y.P., Ramamoorthy, L. and Kumar Ravi, R.V.S.S.N. (2003). Optical absorption spectrum of dysprosium zinc phosphate glass, *Opt. Mat.*, 22, 215-220.
- [28] Meena, S.L. (2021). Spectral and Raman analysis of Sm<sup>3+</sup> ions doped lead lithium potassium niobate borophosphate glasses.
- [29] Meena, S.L. (2020). Spectroscopic properties of Dy<sup>3+</sup> doped lead lithium cadmium tantalum magnesium bismuth borate glasses, *Int. J. of Chem. And Phy. Sci.*, 9(1), 5-12.
- [30] Meena, S.L. (2021). Spectral and Raman analysis of Sm<sup>3+</sup> ions doped zinc lithium cadmium borophosphate glasses, *Int. J. in Phy. And App. Sci.*, 8(4), 7-15.





10.22214/IJRASET



45.98



IMPACT FACTOR:  
7.129



IMPACT FACTOR:  
7.429



# INTERNATIONAL JOURNAL FOR RESEARCH

IN APPLIED SCIENCE & ENGINEERING TECHNOLOGY

Call : 08813907089  (24\*7 Support on Whatsapp)